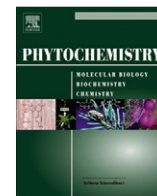




Contents lists available at SciVerse ScienceDirect

Phytochemistry

journal homepage: www.elsevier.com/locate/phytochem

Characterisation of alleles of tomato light signalling genes generated by TILLING

Matthew O. Jones^{a,1}, Florence Piron-Prunier^{b,1}, Fabien Marcel^b, Elodie Piednoir-Barbeau^b, Abdullah A. Alsadon^c, Mahmoud A. Wahb-Allah^c, Abdullah A. Al-Doss^c, Chris Bowler^d, Peter M. Bramley^a, Paul D. Fraser^a, Abdelhafid Bendahmane^{b,*}

^aSchool of Biological Sciences, Royal Holloway, University of London, Egham, Surrey TW20 0EX, United Kingdom

^bUnité de Recherche en Génétique Végétale, UMR INRA-CNRS-Université d'Evry, Evry, France

^cDepartment of Plant Production, College of Food and Agricultural Sciences, King Saud University, Riyadh, Saudi Arabia

^dInstitut de Biologie de l'Ecole Normale Supérieure, Centre National de la Recherche Scientifique, Unité Mixte de Recherche 8197, 75005 Paris, France

ARTICLE INFO

Article history:

Received 29 November 2011

Received in revised form 3 April 2012

Available online xxxxx

Keywords:

Solanum lycopersicum

Solanaceae

Tomato

Mutant phenotyping

Carotenoid

Phenylpropanoid

Photomorphogenesis

ABSTRACT

Targeting Induced Local Lesions IN Genomes (TILLING) combines chemical mutagenesis with high throughput screening to allow the generation of alleles of selected genes. In this study, TILLING has been applied to produce a series of mutations in genes encoding essential components of the tomato light signal transduction pathway in an attempt to enhance fruit nutritional quality. Point mutations to *DEETIOLATED1* (*DET1*), which is responsible for the *high pigment2* (*hp2*) tomato mutant, resulted in elevated levels of both carotenoid and phenylpropanoid phytonutrients in ripe fruit, whilst immature fruit showed increased chlorophyll content, photosynthetic capacity and altered fruit morphology. Furthermore, genotypes with mutations to the *UV-DAMAGED DNA BINDING PROTEIN 1* (*DDB1*), *COP1* and *COP1like* were also characterised. These genotypes largely did not display phenotypes characteristic of mutation to light signalling components but their characterisation has enabled interrogation of structure function relationships of the mutated genes.

© 2012 Elsevier Ltd. All rights reserved.

1. Introduction

Plants offer a diverse mixture of nutrients that are essential for human nutrition and contribute to the promotion of good health. Epidemiological studies show that increased consumption of fruits and vegetables is associated with a reduced risk of several diseases, including cancer and cardiovascular diseases (Key et al., 2002). Carotenoids, flavonoids, phenylpropanoids, tocopherols and ascorbic acid (vitamin C) are all bioactives with potent antioxidant properties and ripe tomato (*Solanum lycopersicum*) fruit are a principal dietary source of each (Giovannucci et al., 2002). In the last decade, genetic manipulation (GM) of light signal transduction components has been an effective means to improve fruit nutritional quality, because it enables simultaneous enhancement of multiple phytonutrients (Davuluri et al., 2005; Enfissi et al., 2010; Liu et al., 2004). To date, transgenic tomato varieties manipulated for *DET1* and *COP1LIKE* gene expression have been produced, resulting in substantial elevations in carotenoid and flavonoid contents in ripe fruit (Davuluri et al., 2005; Enfissi et al., 2010; Liu et al., 2004).

These attempts have followed the isolation of genes responsible for photomorphogenesis mutants in tomato, amongst which are the *high pigment* (*hp*) mutants. These mutants are characterised by an exaggerated responsiveness to light and elevated pigment content resulting in dark green foliage and immature fruit when grown in the light, but do not display an obvious phenotype in darkness (Kendrick et al., 1997). Underlying the phenotype are increases in expression of phenylpropanoid biosynthesis pathway and plastid biogenesis-related transcripts, the latter resulting in increased plastid compartment size (Cookson et al., 2003; Kolotilin et al., 2007; Mustilli et al., 1999).

The monogenic recessive mutants *hp1* and *hp2* are phenotypically identical but genetic analysis of *hp2* revealed mutations in *DEETIOLATED1* (*DET1*) (Mustilli et al., 1999), whilst the *hp1* is a mutation in *DDB1*, which encodes UV-damaged DNA binding protein 1 (Lieberman et al., 2004). Numerous alleles of the *hp1* and *hp2* genes exist (*hp1* and *hp1^w*, *hp2*, *hp2^l* and *hp2^{de}*) (Levin et al., 2003; Lieberman et al., 2004) and double *hp1* and *hp2* mutants display a synergistic phenotype, suggesting association between *DET1* and *DDB1*.

In Arabidopsis, *DDB1* and *DET1* indeed interact. Furthermore, they interact with a third protein, *COP10*, in the *COP10*, *DDB1*, *DET1* (*CDD*) complex (Schroeder et al., 2002; Yanagawa et al., 2004). This complex associates with the E3 ubiquitin ligase *COP1* and the *COP9* signalosome (*CSN*) to promote ubiquitin mediated

* Corresponding author. Tel.: +33 (0)1 60 87 45 02; fax: +33 (0)1 60 87 45 10.

E-mail address: bendahm@evry.inra.fr (A. Bendahmane).

¹ These authors contributed equally to this work.

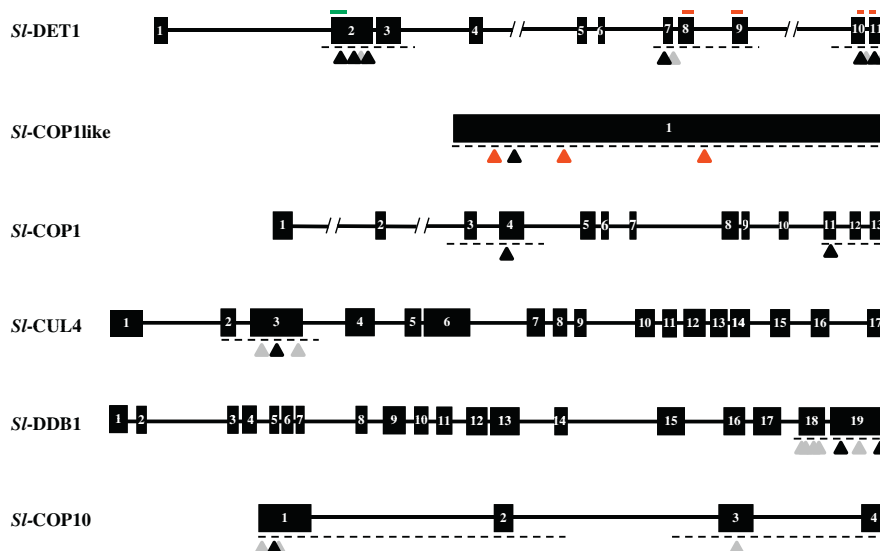


Fig. 1. Representation of exonic induced mutations in *SIDET1*, *SICOP1like*, *SICOP1*, *SICULA*, *SIDDB1*, and *SICOP10* genes. Black boxes represent the exons. Lines linking exons indicate introns. Dashed lines indicate the genomic regions screened for mutations. Red, black and grey triangles represent alterations causing truncations, missense and silent mutations, respectively. Red horizontal bars indicates putative nuclear localization signals. Green horizontal bar indicates the interacting domain to the core circadian clock components, CCA1 (CIRCADIAN CLOCK ASSOCIATED 1) and LHY (LATE ELONGATED HYPOCOTYL, Lau et al., 2011).

degradation of photomorphogenic factors (Osterlund et al., 2000; Yanagawa et al., 2004). Recently, the CDD complex and COP1 were shown to interact with a scaffold protein CULLIN 4 (CUL4) to create two distinct complexes which may act in concert in the regulation of photomorphogenesis (Chen et al., 2006). Further studies proposed a model of tomato DET1 function in regulating gene expression through chromatin remodelling, permitting transcriptional activation of genes in the light (Benvenuto et al., 2002).

High throughput, GM-free techniques to manipulate gene function offer a viable alternative to GM technology that avoids

consumer concerns over the use of GM foodstuffs. TILLING (Targeting Induced Local Lesions IN Genomes) uses ethyl methanesulphonate mutagenesis (EMS) coupled with gene-specific detection of single-nucleotide mutations to generate novel alleles of genes of interest. Due to the availability of genome sequence data, TILLING has found application in reverse genetic studies in a variety of plant species including lotus (*Lotus japonicas*, (Perry et al., 2003)), rice (*Oryza sativa*, (Till et al., 2007)), maize (*Zea mays*, (Till et al., 2004)), wheat (*Triticum aestivum*, (Slade et al., 2005)), pea (*Pisum sativum*, (Dalmais et al., 2008)), soybean (*Glycine max*, (Cooper

Table 1
Mutations discovered in *SI-DET1*, *SI-COP1like*, *SI-COP1*, *SI-CULA*, *SI-DDB1*, *SI-COP10* genes. Only exonic mutations are shown. The position of the mutations is indicated relative to the first base of the GenBank sequences. Silent mutations to amino acids are indicated by =sign.

Gene name	GenBank Accession number	Nucleotide change (position in Genbank accession)	Nucleotide change (position from start of CDS)	Amino acid change	SIFT prediction		
<i>SI-DET1</i>	AJ222798	G321A	G173A	G58D	Not tolerated (0.00)		
		C480T	C332T	T111I	Not tolerated (0.01)		
		C517T	C369T	F123=	-		
		C615T	C467T	P156L	Not tolerated (0.01)		
		G1154A	G1006A	D336N	Tolerated (0.21)		
		C1183T	C1035T	Y345=	-		
		C1559T	C1411T	L471=	-		
		C1578T	C1430T	P477L	Tolerated (0.11)		
		C1611T	C1463T	T488I	Tolerated (0.07)		
		A1657T	A1509T	A503=	-		
		<i>SI-COP1like</i>	AK326710	G417A	G68A	W23Stop	-
				T449A	T100A	L34M	Tolerated (0.22)
				C533T	C184T	Q62Stop	-
G763A	G414A			W138Stop	-		
G643A	G610A			D204N	Tolerated (0.27)		
<i>SI-COP1</i>	AF029984	C1691T	C1658T	A553V	Not tolerated (0.00)		
		<i>SI-CULA</i>	EU218537	A672T	A534T	I178=	-
G735A	G597A			M199I	Not tolerated (0.03)		
G819A	G681A			E227=	-		
<i>SI-DDB1</i>	AY452480	C2496T	C2496T	F832=	-		
		C2506T	C2506T	L836=	-		
		G2544A	G2544A	K848=	-		
		C2680T	C2680T	L894=	-		
		C2854A	C2854A	R952S	Tolerated (0.2)		
		G3007A	G3007A	L1003=	-		
		G3226A	G3226A	V1076I	Tolerated (0.37)		
<i>SI-COP10</i>	AK325615	C46T	C18T	P6=	-		
		G95A	G67A	G23R	-		
		G115A	G87A	S29=	-		
		C406T	C378T	N126=	-		

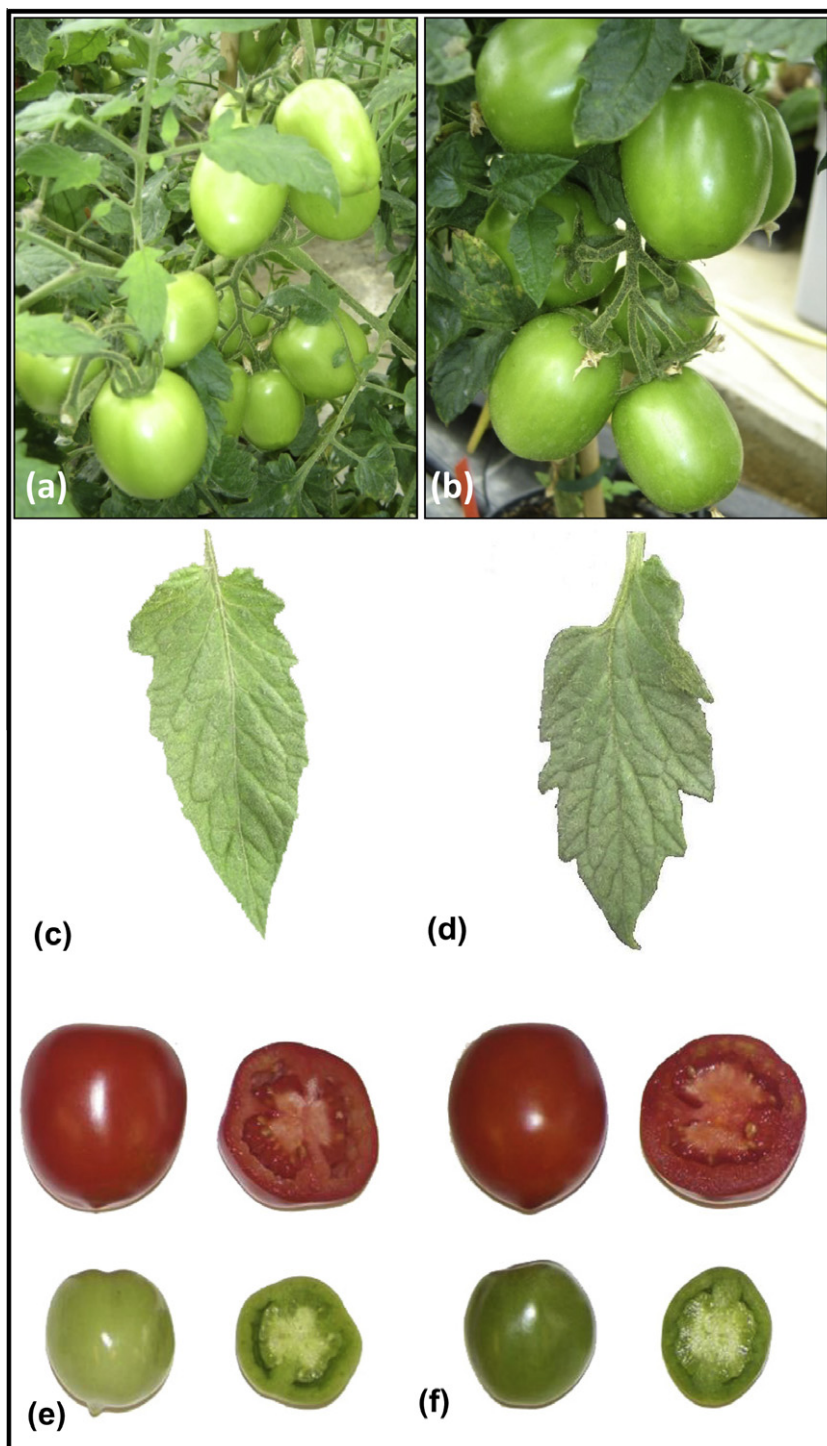


Fig. 2. Fruit and leaf phenotypes of *SI-DET1* C480T mutant. (a) M82 wild type plants. (b) *SI-DET1* C480T mutant plants. Leaves from (c) M82 wild type and (d) *SI-DET1* C480T mutant plants. Immature and mature fruits from (e) M82 wild type and (f) *SI-DET1* C480T mutant plants.

et al., 2008)), and *Brassica rapa* (Stephenson et al., 2010). Here we have used TILLING in tomato to generate new allelic variants of *SI-DET1*, *SI-COP1like*, *SI-COP1*, *SI-CUL4*, *SI-DDB1* and *SI-COP10*, in an attempt to increase fruit nutritional value and better understand the functional importance of different alleles of each gene. The mutant lines were characterized phenotypically and profiled with respect to phenylpropanoid and carotenoid contents. In the case of *SI-DET1* we describe a population of plants with varying degrees of phenotypic aberration, as well as distinct metabolite profiles. The effectiveness of TILLING to phenocopy the natural light signalling

mutants to enhance fruit colour and nutritional quality is discussed.

2. Results and discussion

2.1. EMS mutation screening in *SI-DET1*, *SI-COP1like*, *SI-COP1*, *SI-CUL4*, *SI-DDB1*, *SI-COP10* genes

To test whether new alleles of the photomorphogenesis regulatory DET1 complexes could be engineered by TILLING, the M82

Table 2
Performance index and photosynthetic efficiency of *SI-DET1* and *hp2* mutants expressed as Fv/Fm.

Genotype	Fv/Fm	Performance index
M82	0.833 ± 0.001	3.092 ± 0.104
C480T	0.836 ± 0.002**	4.500 ± 0.249***
MM	0.825 ± 0.002	3.685 ± 0.080
<i>hp2</i> (MM)	0.841 ± 0.002***	6.473 ± 0.262***
<i>hp2^l</i> (MM)	0.841 ± 0.002***	7.059 ± 0.699***

Fv/Fm values were determined from fully expanded leaves using a PAM Pocket Pea, with 10 recordings each taken from three plants per genotype. Values shown in bold are either significantly higher or significantly lower than those of the appropriate background genotype (MM, Moneymaker background for *hp2* and *hp2^l* mutants). The data are presented as means ± SEM. Student's *t*-tests were used to determine significant differences by pair wise comparison between the mutant alleles and their respective wild-type backgrounds.

** *P* < 0.01.

*** *P* < 0.001.

mutant collection (Menda et al., 2004; Piron et al., 2010) was screened for mutations in genes encoding the DET1, COP1like, COP1, CUL4, DDB1 and COP10 proteins. For *SI-COP1like* and *SI-COP10* genes, plants were screened for mutations within exonic regions. For other genes, the focus of screening was on regions predicted by CODDLE (Codons Optimised to Discover Deleterious Lesions) most likely to result in deleterious effects on proteins i.e., exons 2–3 and 7–11 for *SI-DET1*, which contain the interacting domain with core circadian clock components (Lau et al., 2011) and the putative bipartite nuclear localization signal (Mustilli et al., 1999), respectively, as well as exons 3–4 and 11–13 for *SI-COP1*, exons 2–3 for *SI-CUL4*, exons 18 and 19 for *SI-DDB1* (Fig. 1).

TILLING of *SI-DET1* yielded 22 independent point mutations, which corresponded to 12 intronic, four silent and six missense mutations. Table 1 shows the exonic mutations identified for *SI-DET1*, *SI-COP1*, *SI-COP10*, *SI-COP1like*, *SI-CUL4* and *SI-DDB1*. TILLING of *SI-COP1like* yielded four independent point mutations, which correspond to one missense and three stop codon mutations (Table 1). TILLING of *SI-COP1* yielded seven independent mutations, corresponding to two missense mutations. TILLING of *SI-CUL4* yielded three independent point mutations, which correlate to two silent and one missense mutation. TILLING of *SI-DDB1* yielded 10 independent point mutations, which relate to three intronic, five silent and two missense mutations. Finally, TILLING of *SI-COP10* produced 33 independent point mutations, which correspond to twenty nine intronic, three silent and one missense mutation.

For all exonic mutants generated, homozygous lines were obtained from self-pollination of heterozygous mutated lines, except for the *SIDE1* G321A line, for which we were unable to obtain homozygous plants. Germination tests allowed detection of one third wild type and two thirds heterozygous plants, showing that the *SIDE1* G321A homozygous mutated line is affected in

Table 3
Chlorophyll and carotenoid content in mature green fruit of *SI-DET1* mutants.

	DET1 genotypes					
	M82	C480T	C615T	G1154A	C1578T	C1611T
	μg g ⁻¹ DW					
Chlorophyll <i>a</i>	14.8 ± 2.4	45.5 ± 5.9*	26.0 ± 1.7*	11.6 ± 1.8	19.9 ± 3.8	16.0 ± 3.3
Chlorophyll <i>b</i>	99.8 ± 5.9	289.9 ± 45.0*	164.5 ± 10.0**	76.7 ± 12.3	130.3 ± 22.2	129.1 ± 25.4
Chlorophyll <i>a + b</i>	114.5 ± 8.3	335.4 ± 50.7*	190.5 ± 11.6**	88.3 ± 14.1	150.1 ± 25.9	145.1 ± 28.7
Total carotenoid	66.1 ± 8.1	152.5 ± 27.8*	80.2 ± 6.8*	47.2 ± 5.6	76.9 ± 6.2	85.3 ± 10.5
CHL:CAR	1.8 ± 0.2	2.2 ± 0.1	2.2 ± 0.1	2.1 ± 0.1	2.1 ± 0.2	1.7 ± 0.1

Chlorophyll and carotenoid contents are given as μg/g DW and determined as described in the Section 4. Each genotype is represented by three plants, with two or more fruit pooled from each plant. The data are presented as means ± SEM. Student's *t*-tests were used to determine significant differences between TILLed lines and the wild-type control background. CHL, chlorophyll; CAR, carotenoid; DW, dry weight.

* *P* < 0.05.

** *P* < 0.01.

germination (Supplementary Table 1), and this mutation might therefore alter a key amino acid needed for normal protein function. This conclusion is justified by the fact that this mutation is in an interval of 61 amino acids that were shown to be important for the interaction with the core circadian clock components, CCA1 (Circadian Clock Associated 1) and LHY (Late Elongated Hypocotyl) proteins (Lau et al., 2011).

It has previously been suggested that EMS mutagenesis induces exclusively G/C to A/T base transitions due to the mechanism of EMS activity (Greene et al., 2003). Perry and co-workers (2009) reported a frequency of transversions (A/G to T/C) of 2.4% in an EMS mutagenesis *Lotus japonicus* population and concluded that these were due to spontaneous mutations in the genome. Here, we identified 87.5% of G/C to A/T transitions and 12.5% were A/G to T/C transversions.

2.2. The *SI-DET1* mutation affects fruit morphology

The *SI-DET1* C480T plant was first visually phenotyped in the field by Menda et al. (2004), as a small plant with high pigment leaves and fruits. When grown under greenhouse conditions, *SI-DET1* mutants showed more intense leaf colouration than M82 wild type plants, a phenotype most distinct in the *SI-DET1* C480T line (Fig. 2). Fruit were also affected, and colour measurements of mature green fruits recorded significant differences in ΔE for lines *SI-DET1* C480T, C615T, G1154A and C1611T compared to M82 WT fruits, determined according to the colour system L*a*b* (Supplementary Table 2). *SI-DET1* C480T fruit were also smaller than M82 wild type fruit, weighing on average 25% less than M82 wild type fruits at the ripe stage. Ripe fruit weights from the other lines were not statistically different from the M82 wild type fruits. These phenotypes are characteristic of exaggerated light sensitivity and have been reported in the natural high pigment mutants (Kendrick et al., 1997). Furthermore, transgenic manipulations of *SIDE1* by over-expression of mutated *DET1* sequences resulted in a range of plant phenotype severities, including dwarfism and dark green immature fruits (Davuluri et al., 2004).

2.3. Photosynthetic activity and accumulation of chlorophylls is elevated in *DET1* mutants

In order to understand changes in fruit morphology, photosynthetic activity was measured in leaves of *SI-DET1* C480T and M82 wild type plants. Fv/Fm represents the maximum quantum efficiency of photosystem II (PSII) and is a sensitive indicator of photosynthetic performance. Fv/Fm was shown to be significantly elevated in *SI-DET1* C480T. A similar increase in PSII efficiency was also determined for *hp2^l* when compared to its WT background Moneymaker (MM, Table 2). Furthermore, performance index (PI) measurements were calculated, based on the JIP test as

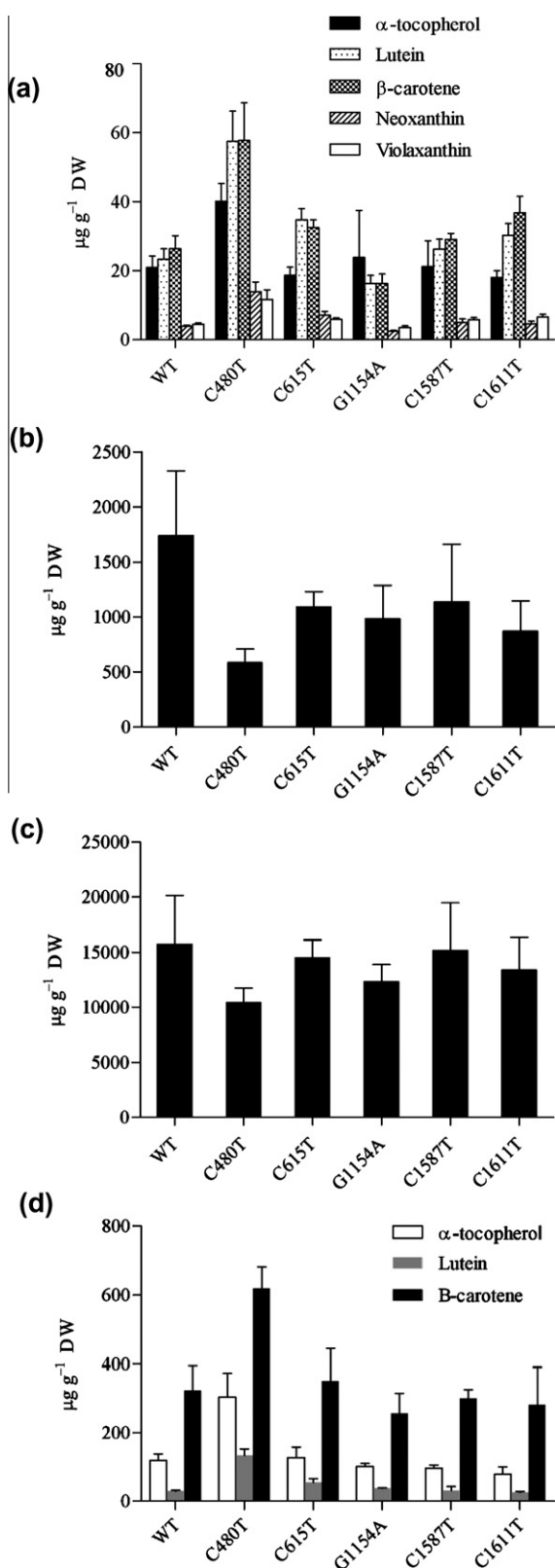


Fig. 3. Isoprenoids in mature green and red ripe fruits of *SI-DET1* mutants. Isoprenoids were extracted from mature green (a) and red ripe (b–d) fruit. (b) phytoene content; (c) lycopene content; (d) α -tocopherol, β -carotene and lutein content. Methods used for determinations are described in Section 4. Two or more fruits from three plants were used for each genotype. Fruits were pooled and three determinations made per sample, to provide three biological and three technical replications. Error bars show \pm SEM. DW, dry weight.

described previously (Strasser et al., 1999). PI is an indicator of plant vitality and combines three parameters favourable to photosynthetic activity: the density of reaction centres; the quantum yield of primary photochemistry and the ability to feed electrons into the electron chain between photosystem II and photosystem I. Each of the *SI-DET1* C480T mutants was shown to have significantly elevated PI values compared to their controls, with *SI-DET1* C480T having an increase of 45% over M82 wild type (Table 2). PI values in *hp*² and *hp*^{2j} were 76% and 92% greater than MM, respectively. These measurements indicate that the *SI-DET1* mutated lines have higher photosynthetic activity than WT and to some extent phenocopy the natural mutants. Increased plastid number and compartment size are major phenotypic traits of the *hp* mutants (Cookson et al., 2003; Kolotilin et al., 2007; Yen et al., 1997) and extensive array analysis of the *high pigment* mutants plants has identified consistent upregulation of transcripts related to plastid biogenesis and photosynthesis. It is known that photosynthesis genes are regulated by signals derived from the nucleus and that this 'retrograde' signalling is important in integrating metabolic pathways and development (Rodermeil, 2001). Furthermore, activation of core metabolic processes in transgenic *SI-DET1* mutants was concluded to be the main effect of loss of DET1 function (Enfissi et al., 2010) and these photosynthetic measurements support that interpretation. Of the *SI-COP1Like*, *SI-COP10* and *SI-DDB1* mutants, only *SI-COP1Like* G763A was significantly different from its background genotype, having elevated Fm/Fm and PI values (Supplementary Table 3).

Another phenotypic trait of the *hp*² mutant is an increased accumulation of chlorophyll (Kerckhoffs et al., 1997). Chlorophyll levels were determined for all five *SI-DET1* homozygous lines at the mature green stage of fruits development. All lines except the *SI-DET1* G1154A line showed statistically significant increases in chlorophylls *a* and *b*, compared to M82 wild type fruits (Table 3). Combined chlorophyll *a* and *b* contents were up to three-fold greater in *SI-DET1* C480T line, with levels of $335.4 \mu\text{g g}^{-1}$ DW (Table 3), confirming the visual phenotype. This elevation is within the range observed in *hp-2* mutants and *SI-DET1* RNAi transgenic lines (Enfissi et al., 2010).

2.4. *SI-DET1* mutations affect carotenoid levels

In agreement with chlorophyll levels, carotenoid content was also elevated at the mature green stage of development. This was evident in fruits from all lines excluding *SI-DET1* G1154A, which show a reduction in total carotenoid content of 34% (Fig. 3a). Notably, no change in the carotenoid composition was observed in the *SI-DET1* homozygous lines, with the relative increases among individual carotenoids and xanthophylls and the ratio of chlorophylls to carotenoids being largely unchanged. This phenomenon has been previously observed in response to *SI-DET1* gene silencing, where three transgenic varieties each had similar chlorophyll to carotenoid ratios, despite great variations in total pigment contents (Enfissi et al., 2010). In contrast to this, in ripe fruits, *SI-DET1* C480T shows a distinct carotenoid profile compared to the M82 wild type fruits that indicated an increased flux through the carotenoid pathway. Levels of phytoene, the first C₄₀ carotenoid, and lycopene were both significantly reduced (Fig. 3b and c), whilst levels of β -carotene (1.9-fold) and lutein (4.5-fold) were both increased in this genotype, *SI-DET1* C480T. In addition, there is an increase in α -tocopherol (Fig. 3d). Mutants of *SI-DDB1*, *SI-COP1like* and *SI-COP10* were also profiled. At the mature green stage there were no significant differences between the homozygous mutants and their respective background genotypes, with the exception of a reduction in neoxanthin in *SI-COP1like* G763A mutant (Supplementary Table 4). In red ripe fruit there were reductions in phytoene and lutein in *SI-DDB1* C2854A and

Table 4
Phenolic content of *Sl-DET1* fruit at mature green and red ripe stages.

	M82	C480T	C615T	G1154A	C1578T	C1611T
	$\mu\text{g g}^{-1}$ DW					
<i>Sl-DET1</i> genotypes mature green						
Chlorogenic acid	21.0 \pm 5.9	39.5 \pm 1.9*	21.8 \pm 9.1	24.0 \pm 6.7	38.5 \pm 6.9	37.2 \pm 10.2
Rutin	21.3 \pm 4.6	46.3 \pm 5.0*	15.1 \pm 3.2	26.3 \pm 3.1	31.6 \pm 7.8	23.2 \pm 5.9
<i>Sl-DET1</i> genotypes red ripe						
Caffeic acid	2.3 \pm 0.6	11.1 \pm 1.3**	6.7 \pm 2.4	3.7 \pm 0.8	3.0 \pm 0.7	4.7 \pm 2.6
Ferulic acid total	12.5 \pm 1.5	59.9 \pm 11.5*	33.4 \pm 8.8	15.0 \pm 1.7	15.3 \pm 1.2	19.4 \pm 8.5
Chlorogenic acid total	28.6 \pm 3.9	51.5 \pm 10.6	40.4 \pm 4.8	23.5 \pm 6.3	26.1 \pm 2.9	30.3 \pm 9.3
Chalcone naringenin	58.3 \pm 9.9	38.8 \pm 14.8	68.0 \pm 23.2	86.3 \pm 10.1	51.2 \pm 23.4	60.6 \pm 21.6
Naringenin	10.8 \pm 2.5	8.8 \pm 0.6	11.5 \pm 2.4	10.7 \pm 2.1	8.2 \pm 1.9	9.6 \pm 1.6
Rutin total	27.0 \pm 7.6	61.7 \pm 15.8	34.0 \pm 11.4	16.7 \pm 2.6	22.7 \pm 5.9	21.1 \pm 7.0

Contents are given as $\mu\text{g/g}$ DW and determined relative to a salicylic internal standard as described in the Section 4. Each genotype is represented by three plants, with two or more fruits pooled from each plant. The data are presented with \pm SEM. Student *t*-tests were used to determine significant differences between respective wild type background and transgenic varieties. DW, dry weight.

* $P < 0.05$.

** $P < 0.01$.

G3226A lines respectively, and reductions in β -carotene and α -tocopherol in *Sl-DDB1* A3164T (Supplementary Table 5).

2.5. Analysis of phenolics

The phenylpropanoids caffeic acid, ferulic acid and chlorogenic acid, and the flavonoids chalcone naringenin, naringenin and rutin were analysed in fruit samples. Compared to wild type mature green fruits, *Sl-DET1* the C480T mutant showed an increase in chlorogenic acid and rutin level of 1.9- and 2.2-fold, respectively (Table 4). The most dramatic changes at the ripe stage were also detected in *Sl-DET1* C480T, which contained 8.5-fold greater ferulic acid levels and 4.8 fold greater caffeic acid levels (Table 4), and confirmed the visual phenotype of the fruit. Among the *Sl-DDB1*, *Sl-COP1like* and *Sl-COP10* mutant lines, the only substantial relative differences recorded in ripe fruits were a 2.5-fold increase in caffeic acid levels in *Sl-DDB1* C2854A and a 3.5-fold reduction in chalcone naringenin for *Sl-COP1like* G763A mutant (Supplementary Tables 6 and 7).

2.6. Principal component analysis of steady state metabolite concentrations

Metabolite profiling using GC-MS was used to identify and quantify over forty metabolites from each *Sl-DET1* mutated lines and M82 wild type plants in mature green and ripe fruits. Multivariate principal component analysis (PCA) was applied to the two data sets. PCA separates samples on the basis of the cumulative correlation of all metabolite data and identifies those components that provide the greatest separation between samples. At the mature green stage, scatter plots of components one and three showed the clearest groupings of the genotypes and demonstrate that the novel *Sl-DET1* alleles are sufficiently different to generate fruits with distinct metabolic profiles, as shown in Fig. 4a. Three of the *Sl-DET1* TILLed lines constituted distinct single clusters, away from M82 wild type, whilst the remaining genotypes showed greater separation of individual plant replicates than for different genotypes. *Sl-DET1* C480T and *Sl-DET1* C1611T separated furthest from the control. Analysis of the loadings, which define the major determinants of the separation, revealed that sugars and organic acids contributed to separation in the PC-1 dimension, whilst the amino acids glycine, valine and threonine were found in the negative sector of PC-3. Mature green fruits from *Sl-DET1* C480T contained elevated levels of succinic acid and reduced levels of citric acid, linoleic and palmitic acids. Among the sugars, *Sl-DET1*

C480T contained an increase in maltose and xylose but reductions in arabinose, sucrose and glucose.

Separation among genotypes was less distinct in ripe fruits; nonetheless *Sl-DET1* C480T, *Sl-DET1* C615T and *Sl-DET1* C1578T genotypes did separate into clusters distinct from M82 WT (Fig. 4b). Most separation was observed in the PC-1 dimension, in which the organic acids oxalic, galacturonic and quinic were present in the negative sector. In the positive sector of PC-1, sugars glucose, fructose and xylose were present in addition to a number of amino acids. There were consistent decreases in the amino acids threonine and alanine in all *Sl-DET1* varieties, but the majority of metabolites were differentially affected in different varieties. Levels of oxalic acid, for example, were reduced by 89% and 60% in C480T and C615T, respectively, when compared to levels in M82, but unchanged or increased in the remaining three varieties. Nonetheless, these findings provide evidence of perturbation to core metabolic processes in our mutants.

2.7. Comparison of *DET1*, *DDB1*, *COP1like* and *COP10* mutants

Of the 25 exonic mutations to *Sl-DET1*, *Sl-DDB1*, *Sl-COP1like* and *Sl-COP10*, 10 (40%) were missense (resulting in amino acid changes), three result in truncation (12%, mutations to nonsense codons), and 12 (48%) were silent mutations. This distribution is similar to the proportions of missense (50%) truncation (5%) and silent (45%) reported previously in a large scale Arabidopsis screen (Till et al., 2003). Among these, only the *Sl-DET1* C480T mutant showed dark green fruits and substantial alteration to pigment content, despite the similarities between the *hp1* (*DDB1*) and *hp2* (*DET-1*) mutants. To understand this observation, the functional consequences of the amino acid substitutions generated by TILLING need to be considered. A nonsynonymous single nucleotide polymorphism (nsSNP) or missense variant is a single base change that introduces an amino acid polymorphism into a protein and it is understood that these are more likely to be deleterious to protein function if they occur at positions that are conserved throughout evolution (Miller and Kumar, 2001). Similarly there is an intolerance to mutations at residues confined to particular classes of amino acids (Bowie et al., 1990; Markiewicz et al., 1994), suggesting that changes to protein structure, affected by residue rigidity, hydrophobicity and volume, may also be used to predict whether an amino acid substitution will affect protein function. The SIFT program (Ng and Henikoff, 2001) was used to make predictions of all the alleles generated. SIFT predicted three nonsynonymous mutations to *DET1* which could not be tolerated (*Sl-DET1* G321A, C480T and C615T). The G to A transition at

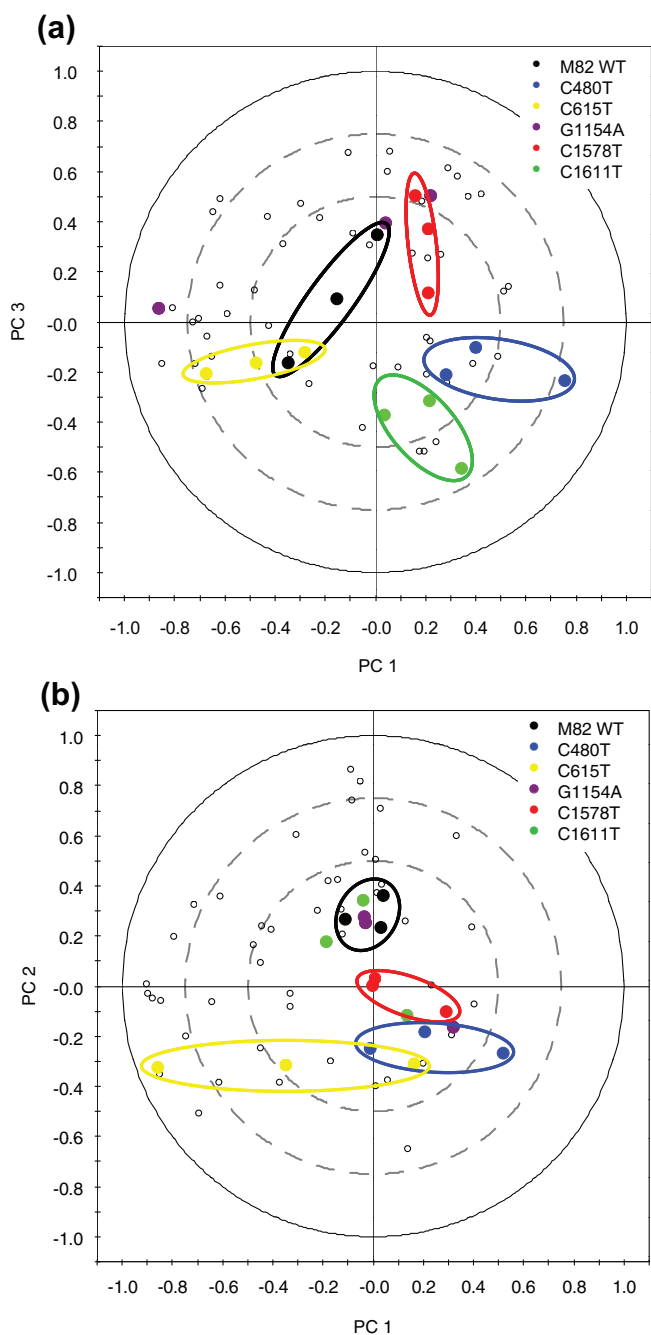


Fig. 4. PCA of the metabolite profiles of *SI-DET1* TILLED and WT fruits. (a) Mature green fruits. Vectors 1 and 3 were chosen to provide the best visualisation of differences between genotypes, which were responsible for 18% and 10% of the total variance, respectively. (b) Red ripe fruits. Vectors 1 and 2 were chosen to give the best sample separation and represented 20% and 15% of total variance, respectively. In each plot, each genotype is represented by three plants with two to three fruits per plant. Genotype replicates are shown by coloured dots, with each dot representing a combination of all metabolites from an individual sample. Loadings are shown as empty circles. Ellipses have been overlaid to aid the clustering of specific genotypes.

position 321 resulted in substitution with aspartic acid of a glycine residue conserved across plant and human DET1 proteins and therefore likely to be crucial for protein function. This modification had a SIFT score of 0.00 (Table 1), predictive of very substantial effect and the homozygous mutation was lethal (Supplementary Table 1). The *SI-DET1* C480T mutation, the strongest *SI-DET1* allele is a substitution of a polar threonine residue to nonpolar isoleucine

at amino acid 111. Although this residue is not conserved with *Arabidopsis* DET1, its substitution was sufficient to affect protein function, resulting in a characteristic *high pigment* phenotype. Both the *hp2* and *hp2^l* mutants affect exon 11 at the C-terminus of the DET1 protein (Mustilli et al., 1999). In *hp2^l*, a substitution of a conserved proline for a serine residue at amino acid 498, and the *hp2* mutant results in deletion of glycine, proline and glutamine at the start of exon 11.

The nature of amino acid substitutions in the *SI-DDB1* gene can explain why only mild differences in fruit phenotype and metabolite content were detected in the lines produced. Although the mutations affect amino acids conserved across DDB sequences from other plant species, the substitutions were conservative and did not result in substantial changes in charge. *SI-DDB1* C2854A mutation causes a substitution of arginine (positive) to serine (neutral); *SI-DDB1* A3164T: glutamic acid (negative) to valine (neutral) and *SI-DDB1* G3226A valine (neutral) to isoleucine (neutral). This contrasts with the *hp1^w* mutation, caused by a single G to A resulting in substitution of an acidic residue, glutamic acid, for the basic residue lysine at position 798 (Lieberman et al., 2004).

Unlike the *SI-DDB1* alleles, the mutations to *SI-COP1*like resulted in protein truncation: G417A (tryptophan to stop), T449A (leucine, neutral, to methionine, neutral), C533T (glutamine to stop) and G793A (tryptophan to stop) and as such may be anticipated to have substantial impact on protein function. In *Arabidopsis*, mutation to the COP1 gene results in constitutive photomorphogenesis and anthocyanin accumulation in weak alleles and is lethal in null mutants (McNellis et al., 1994). In tomato, Liu and co-workers (2008) repressed expression of *SI-COP1*like using RNAi and this resulted in plants with dark green leaves and fruits concomitant with up to 43% greater total carotenoid content. The *SI-COP1*like mutants did not exhibit such phenotypes and one possible explanation is that there is redundancy in the function of *SI-COP1*like and the RNAi construct used previously also affected other proteins with the WD-repeat domain found in *SI-COP1*like. The COP1 protein contains an amino-terminal zinc Ring finger domain, a coiled coil domain, a central core domain and at the carboxy-terminal a domain of WD-40 repeats (Stacey et al., 1999). Evidence from mutant alleles indicates that the COP1 protein consists of two separate functional modules, with the carboxy terminal (COP1C) operating to repress photomorphogenesis, whilst the amino terminal (COP1N) module confers growth and development functions (McNellis et al., 1994, 1996; Stacey et al., 2000). The *SI-COP1*like protein contains the WD40 motif, but since it does not have the other structural domains it is feasible it does not perform the same function as the complete COP1 protein, but may plausibly act in a similar role as COP1C. Further investigation of COP1 and COP1like in tomato are necessary to better understand their roles in regulating photomorphogenesis.

3. Conclusions

These findings demonstrate the effectiveness of TILLING to generate novel allelic series for the genetic improvement of nutritional quality in tomato. The mutants presented each resulted in phenotypes of different severity and as such they provide an opportunity to assess the functional importance of the substituted amino acids. The *SI-DET1* mutants largely phenocopied the well studied *hp2* and *hp2^l* mutants, and we have extended their characterisation by recording enhanced photosynthetic performance as measured by fluorescence parameters, whilst our *SI-DDB1* mutations did not phenocopy the *hp1* mutant. Genetic crosses between mutants affected in *SI-DET1*, *SI-COP1*like and *SI-DDB1* have been performed which will enable the generation of potentially stronger high pigment phenotypes.

4. Experimental

4.1. Materials

The mutagenised M82 population composed of 4759 M3 families was used, mutagenised with 0.7% ethyl methanesulphonate (Piron et al., 2010). Plants were glasshouse grown from seed under supplementary lighting. Three plants per genotype were grown in a randomized manner concurrently with their respective backgrounds and fruit harvested at mature green and red ripe stages.

4.2. Accession numbers

The GenBank accession numbers of sequences for TILLING are: AJ222798 (*SI-DET1*); AF029984 (*SI-COP1*); AK325615 (*SI-COP10*); AK326710 (*SI-COP1like*); EU218537 (*SI-CUL4*), and AY452480 (*SI-DDB1*).

4.3. PCR amplification and mutation detection

Young leaves were harvested for genomic DNA extraction using the DNeasy®96PlantKit (Qiagen). PCR amplification procedure was based on nested-PCR whereby the first PCR amplification was a standard PCR reaction using target-specific primers and 4 ng of tomato genomic DNA. Primers used to amplify genes of interest are shown in [Supplementary Table 8](#). One microlitre of the first PCR served as a template for the second nested PCR amplification, using gene-specific inner primers labelled at the 5' end with infra-red dyes IRD700 and IRD800, LI-COR®, Lincoln, Nebraska, USA). Mutation detection was carried out using the EndoI protocol as described previously (Triques et al., 2007). The identity of the mutations was determined by sequencing.

4.4. Germination test

Plants grown on soil for at least two weeks, in a culture chamber under 12/12 h (light/dark) photoperiod at 26 °C. Plants were subsequently screened as described in Section 4.3.

4.5. Analysis of carotenoids and isoprenoids

Each genotype was represented by three individual plants and from each plant multiple fruits were pooled for each developmental stage. Material was freeze dried and 10–20 mg aliquots were used for metabolite analyses. Carotenoid and isoprenoid analyses were performed by HPLC as described in [Enfissi et al. \(2010\)](#). Each treatment was analysed in triplicate. Identification was performed by cochromatography and comparison of spectral properties with authentic standards and reference spectra, and quantification was performed by comparison of integrated peak areas with dose–response curves constructed from authentic standards.

4.6. Analysis of phenolics

Phenylpropanoids were extracted in methanol supplemented with salicylic acid (final concentration 0.04 mg/ml) as an internal standard. Extracts were analysed by HPLC as described in [Enfissi et al. \(2010\)](#). Relative quantification was carried out by comparison of integrated peak areas with the internal standard at the λ_{max} of the phenylpropanoids and flavonoids detected.

4.7. Gas chromatography–mass spectrometry analysis of metabolites

Ground, freeze dried material was extracted in methanol (1 ml; HPLC grade) supplemented with internal standard ribitol (to a

concentration of 0.04 mg/ml). Each genotype was represented by three plants, with two or more fruits per plant, pooled to provide one replicate per plant. Samples were mixed vigorously and then incubated at room temperature for 30 min with continuous agitation. Samples were centrifuged to remove cell debris. Samples were centrifuged at 12,000 rpm for 2 min and the supernatant was removed. From each sample an aliquot (100 μ l) was removed and dried completely under nitrogen gas. Derivatisation was performed by the addition of 50 μ l methoxyamine–HCl (Sigma–Aldrich) prepared at a concentration of 20 mg/ml in pyridine. Samples were incubated at 50 °C for 4 h, after which 80 μ l *N*-methyltrimethylsilyltrifluoroacetamide (Macherey Nagel) was added and the samples incubated for 30 min at 37 °C before analysis. GC–MS analyses were performed as described earlier ([Enfissi et al., 2010](#)), using both a 20:1 and 200:1 split injector.

4.8. Colour determination

Fruit colour was determined according to the colour system CIE $L^*a^*b^*$ colour difference ΔE using a MiniScan XE Plus (HunterLab, Reston, Virginia) calibrated with a white tile. Three measurements were made for each fruit, with ten or more fruits measured each at mature green and ripe stages for all genotypes.

4.9. Photosynthesis measurements

Chlorophyll *a* fluorescence kinetics were measured in six-week old plants under normal glasshouse conditions. Intact, expanding leaves were dark adapted for 10 min prior to fluorescence emission being induced by a saturating illumination of 3500 μ mol $m^{-2} s^{-1}$ (peak 627 nm) for a duration of 1 s using a hand held Pocket PEA (Hansatech instruments). Ten measurements were taken from each plant, with three plants per genotype. The maximum efficiency of PSII photochemistry in the dark-adapted state (Fv/Fm) was determined from the Chl *a* polyphasic fluorescence transient O–J–I–P. Performance index based on the JIP-test was calculated as described previously ([Strasser et al., 1999](#)) Both Fv/Fm and PI were calculated by the PEA Plus software (Hansatech Instruments).

4.10. Data processing and statistical treatment

All experiments typically used a minimum of three biological and three technical replicates, unless stated otherwise. Student's *t*-tests were used to determine significant differences between pairwise comparisons among the different *DET1* TILLED genotypes with the M82 control (WT) and *SI-COP1Like*, *SI-COP1* and *SI-DDB1* genotypes with their respective controls. Graphs were prepared using GraphPad software. Principal component analyses (PCA) were performed using the statistical software package SIMCA-P+12.0 (Umetrics). Analyses are presented as two dimensional scatterplots containing both components and loading contributions. Ellipses were manually overlaid to aid the clustering of selected genotypes.

Acknowledgments

This work was supported by ANR–BBSRC SysBio BB/F005644/1 (M.O.J, P-P.F., F.M., C.B, P.M.B., P.D.F., A.B.), the EUSOL program and the INRA–KSU Plant biotechnology. We thank the TGRC for the supply of *hp* mutant seeds.

Appendix A. Supplementary data

Supplementary data associated with this article can be found, in the online version, at <http://dx.doi.org/10.1016/j.phytochem.2012.04.005>.

References

- Benvenuto, G., Formiggini, F., Laflamme, P., Malakhov, M., Bowler, C., 2002. The photomorphogenesis regulator DET1 binds the amino-terminal tail of histone H2B in a nucleosome context. *Curr. Biol.* 15, 1529–1534.
- Bowie, J.U., Reidhaar-Olson, J.F., Lim, W.A., Sauer, R.T., 1990. Deciphering the message in protein sequences: tolerance to amino acid substitutions. *Science* 247, 1306–1310.
- Chen, H., Shen, Y., Tang, X., Yu, L., Wang, J., Guo, L., Zhang, Y., Zhang, H., Feng, S., Strickland, E., Zheng, N., Deng, X.W., 2006. *Arabidopsis* CULLIN4 forms an E3 ubiquitin LIGASE with RBX1 and the CDD complex in mediating light control of development. *Plant Cell* 18, 1991–2004.
- Cookson, P.J., Kiano, J.W., Shipton, C.A., Fraser, P.D., Romer, S., Schuch, W., Bramley, P.M., Pyke, K.A., 2003. Increases in cell elongation, plastid compartment size and phytoene synthase activity underlie the phenotype of the *high pigment-1* mutant of tomato. *Planta* 217, 896–903.
- Cooper, J.L., Till, B.J., Laport, R.G., Darlow, M.C., Kleffner, J.M., Jamai, A., El-Mellouki, T., Liu, S., Ritchie, R., Nielsen, N., Bilyeu, K.D., Meksem, K., Comai, L., Henikoff, S., 2008. TILLING to detect induced mutations in soybean. *BMC Plant Biol.* 8, 9.
- Dalmats, M., Schmidt, J., Le Signor, C., Moussy, F., Burstin, J., Savoie, V., Aubert, G., Brunaud, V., de Oliveira, Y., Guichard, C., Thompson, R., Bendahmane, A., 2008. UTILLdb, a *Pisum sativum* *in silico* forward and reverse genetics tool. *Genome Biol.* 9, R43.
- Davuluri, G.R., van Tuinen, A., Fraser, P.D., Manfredonia, A., Newman, R., Burgess, D., Brummell, D.A., King, S.R., Palys, J., Uhlig, J., Bramley, P.M., Pennings, H.M., Bowler, C., 2005. Fruit-specific RNAi-mediated suppression of *DET1* enhances carotenoid and flavonoid content in tomatoes. *Nat. Biotechnol.* 23, 890–895.
- Davuluri, G.R., van Tuinen, A., Mustilli, A.C., Manfredonia, A., Newman, R., Burgess, D., Brummell, D.A., King, S.R., Palys, J., Uhlig, J., Pennings, H.M.J., Bowler, C., 2004. Manipulation of *DET1* expression in tomato results in photomorphogenic phenotypes caused by post-transcriptional gene silencing. *Plant J.* 40, 344–354.
- Enfissi, E.M., Barneche, F., Ahmed, I., Lichtle, C., Gerrish, C., McQuinn, R.P., Giovannoni, J.J., Lopez-Juez, E., Bowler, C., Bramley, P.M., Fraser, P.D., 2010. Integrative transcript and metabolite analysis of nutritionally enhanced *DEETIOLATED1* downregulated tomato fruit. *Plant Cell* 22, 1190–1215.
- Giovannucci, E., Rimm, E.B., Liu, Y., Stampfer, M.J., Willett, W.C., 2002. A prospective study of tomato products, lycopene, and prostate cancer risk. *J. Natl. Cancer Inst.* 94, 391–398.
- Greene, E.A., Codomo, C.A., Taylor, N.E., Henikoff, J.G., Till, B.J., Reynolds, S.H., Enns, L.C., Burtner, C., Johnson, J.E., Odden, A.R., Comai, L., Henikoff, S., 2003. Spectrum of chemically induced mutations from a large-scale reverse-genetic screen in *Arabidopsis*. *Genetics* 164, 731–740.
- Kendrick, R.E., Kerckhoffs, L.H.J., Van Tuinen, A., Koornneef, M., 1997. Photomorphogenic mutants of tomato. *Plant Cell Environ.* 20, 746–751.
- Kerckhoffs, L.H.J., De Groot, N.A.M.A., Van Tuinen, A., Schreuder, M.E.L., Nagatani, A., Koornneef, M., Kendrick, R.E., 1997. Physiological characterization of exaggerated-photoreponse mutants of tomato. *J. Plant Physiol.* 150, 578–587.
- Key, T.J., Allen, N.E., Spencer, E.A., Travis, R.C., 2002. The effect of diet on risk of cancer. *Lancet* 360, 861–868.
- Kolotilin, I., Koltai, H., Tadmor, Y., Bar-Or, C., Reuveni, M., Meir, A., Nahon, S., Shlomo, H., Chen, L., Levin, I., 2007. Transcriptional profiling of high pigment-2dg mutant links early fruit plastid biogenesis with its overproduction of phytonutrients. *Plant Physiol.* 145, 389–401.
- Lau, O.S., Huang, X., Charron, J.B., Lee, J.H., Li, G., Deng, X.W., 2011. Interaction of *Arabidopsis* DET1 with CCA1 and LHY in mediating transcriptional repression in the plant circadian clock. *Mol. Cell* 43, 703–712.
- Levin, I., Frankel, P., Gilboa, N., Tanny, S., Lalazar, A., 2003. The tomato *dark green* mutation is a novel allele of the tomato homolog of the *DEETIOLATED1* gene. *Theor. Appl. Genet.* 106, 454–460.
- Lieberman, M., Segev, O., Gilboa, N., Lalazar, A., Levin, I., 2004. The tomato homolog of the gene encoding UV-damaged DNA binding protein 1 (DDB1) underlined as the gene that causes the *high pigment-1* mutant phenotype. *TAG. Theor. Appl. Genet.* 108, 1574–1581.
- Liu, Y., Roof, S., Ye, Z., Barry, C., van Tuinen, A., Vrebalov, J., Bowler, C., Giovannoni, J., 2004. Manipulation of light signal transduction as a means of modifying fruit nutritional quality in tomato. *Proc. Natl. Acad. Sci. USA* 101, 9897–9902.
- Markiewicz, P., Kleina, L.G., Cruz, C., Ehret, S., Miller, J.H., 1994. Genetic studies of the lac repressor. XIV. Analysis of 4000 altered *Escherichia coli* lac repressors reveals essential and non-essential residues, as well as “spacers” which do not require a specific sequence. *J. Mol. Biol.* 240, 421–433.
- McNellis, T.W., Torii, K.U., Deng, X.W., 1996. Expression of an N-terminal fragment of COP1 confers a dominant-negative effect on light-regulated seedling development in *Arabidopsis*. *Plant Cell* 8, 1491–1503.
- McNellis, T.W., von Arnim, A.G., Araki, T., Komeda, Y., Misera, S., Deng, X.W., 1994. Genetic and molecular analysis of an allelic series of *cop1* mutants suggests functional roles for the multiple protein domains. *Plant Cell* 6, 487–500.
- Menda, N., Semel, Y., Peled, D., Eshed, Y., Zamir, D., 2004. *In silico* screening of a saturated mutation library of tomato. *Plant J.* 38, 861–872.
- Miller, M.P., Kumar, S., 2001. Understanding human disease mutations through the use of interspecific genetic variation. *Human Mol. Genet.* 10, 2319–2328.
- Mustilli, A.C., Fenzi, F., Ciliento, R., Alfano, F., Bowler, C., 1999. Phenotype of the tomato *high pigment-2* mutant is caused by a mutation in the tomato homolog of *DEETIOLATED1*. *Plant Cell* 11, 145–157.
- Ng, P.C., Henikoff, S., 2001. Predicting deleterious amino acid substitutions. *Genome Res.* 11, 863–874.
- Osterlund, M.T., Hardtke, C.S., Wei, N., Deng, X.W., 2000. Targeted destabilization of HY5 during light-regulated development of *Arabidopsis*. *Nature* 405, 462–466.
- Perry, J.A., Wang, T.L., Welham, T.J., Gardner, S., Pike, J.M., Yoshida, S., Parniske, M., 2003. A TILLING reverse genetics tool and a web-accessible collection of mutants of the legume *Lotus japonicus*. *Plant Physiol.* 131, 866–871.
- Piron, F., Nicolai, M., Minoia, S., Piednoir, E., Moretti, A., Salgues, A., Zamir, D., Caranta, C., Bendahmane, A., 2010. An induced mutation in tomato eIF4E leads to immunity to two potyviruses. *PLoS one* 5, e11313.
- Rodermerl, S., 2001. Pathways of plastid-to-nucleus signaling. *Trends Plant Sci.* 6, 471–478.
- Schroeder, D.F., Gahrz, M., Maxwell, B.B., Cook, R.K., Kan, J.M., Alonso, J.M., Ecker, J.R., Chory, J., 2002. De-etiolated 1 and damaged DNA binding protein 1 interact to regulate *Arabidopsis* photomorphogenesis. *Curr. Biol.* 12, 1462–1472.
- Slade, A.J., Fuerstenberg, S.I., Loeffler, D., Steine, M.N., Facciotti, D., 2005. A reverse genetic, nontransgenic approach to wheat crop improvement by TILLING. *Nat. Biotechnol.* 23, 75–81.
- Stacey, M.G., Hicks, S.N., von Arnim, A.G., 1999. Discrete domains mediate the light-responsive nuclear and cytoplasmic localization of *Arabidopsis* COP1. *Plant Cell* 11, 349–364.
- Stacey, M.G., Kopp, O.R., Kim, T.H., von Arnim, A.G., 2000. Modular domain structure of *Arabidopsis* COP1: reconstitution of activity by fragment complementation and mutational analysis of a nuclear localization signal in *Planta*. *Plant Physiol.* 124, 979–989.
- Stephenson, P., Baker, D., Girin, T., Perez, A., Amoah, S., King, G.J., Ostergaard, L., 2010. A rich TILLING resource for studying gene function in *Brassica rapa*. *BMC Plant Biol.* 10, 62.
- Strasser, M.G., Srivastava, A., Tsimilli-Michael, M., 1999. Screening the Vitality and Photosynthetic Activity of Plants by Fluorescence Transient. In: Behl, R.K., Punia, M.S., Lather, B.P.S. (Eds.), *Crop Improvement for Food Security SSARM*. Hisar, India, pp. 72–115.
- Till, B.J., Cooper, J., Tai, T.H., Colowit, P., Greene, E.A., Henikoff, S., Comai, L., 2007. Discovery of chemically induced mutations in rice by TILLING. *BMC Biol.* 7, 19.
- Till, B.J., Reynolds, S.H., Greene, E.A., Codomo, C.A., Enns, L.C., Johnson, J.E., Burtner, C., Odden, A.R., Young, K., Taylor, N.E., Henikoff, J.G., Comai, L., Henikoff, S., 2003. Large-scale discovery of induced point mutations with high-throughput TILLING. *Genome Res.* 13, 524–530.
- Till, B.J., Reynolds, S.H., Weil, C., Springer, N., Burtner, C., Young, K., Bowers, E., Codomo, C.A., Enns, L.C., Odden, A.R., Greene, E.A., Comai, L., Henikoff, S., 2004. Discovery of induced point mutations in maize genes by TILLING. *BMC Plant Biol.* 4, 12.
- Triques, K., Sturbois, B., Gallais, S., Dalmais, M., Chauvin, S., Clepet, C., Aubourg, S., Rameau, C., Caboche, M., Bendahmane, A., 2007. Characterization of *Arabidopsis thaliana* mismatch specific endonucleases: application to mutation discovery by TILLING in pea. *Plant J.* 51, 1116–1125.
- Yanagawa, Y., Sullivan, J.A., Komatsu, S., Gusmaroli, G., Suzuki, G., Yin, J., Ishibashi, T., Saijo, Y., Rubio, V., Kimura, S., Wang, J., Deng, X.W., 2004. *Arabidopsis* COP10 forms a complex with DDB1 and DET1 *in vivo* and enhances the activity of ubiquitin conjugating enzymes. *Genes Dev.* 18, 2172–2181.
- Yen, H.C., Shelton, B.A., Howard, L.R., Lee, S., Vrebalov, J., Giovannoni, J.J., 1997. The tomato high-pigment (hp) locus maps to chromosome 2 and influences plastome copy number and fruit quality. *Theor. Appl. Genet.* 95, 1069–1079.